

# Dual-Band SIW Slot Array Filtering Antenna for X and Ku Band Applications

Ayyadevara M. V. N. Maruti\* and Bhavan S. Naga Kishore

**Abstract**—In this work, a substrate integrated waveguide slot array filtering antenna for dual band applications is presented. This novel design performs the functions of both a filter and an antenna simultaneously. The main intention of this work is to design a circuit that separates the frequencies in a dual band operation. The antenna is designed as an integration of two parts; the upper part operates at 10.2 GHz while the lower part operates at 16.4 GHz. In each part, an array of five longitudinal slots is incorporated, as well as a SIW antenna with complementary split ring resonators that operate as a band pass filter at the front end. Each slot array antenna is designed for a specific frequency band, and its function depends upon its preceding band pass filter. The two band pass filters allow only signals from the frequency bands for which they are designed to their corresponding slot array antennas. This technique, along with properly spaced metal vias of the SIW antenna, prevents any leakage and hence reduces interference in dual band operation. Both the band pass filter and the antenna can be built on the same planar board. The antenna is fed through a microstrip to SIW taper transition. CST Microwave Studio software is used for optimization and simulation of the structure. The antenna was built on an RT Duroid 5880 and tested to investigate practical validation. The antenna has a bandwidth of 1.9 GHz, from 9.2 GHz to 11.1 GHz in the X-band, and 2.2 GHz, from 15.6 GHz to 16.9 GHz in the Ku band. The gain pattern is unidirectional in nature and has low side lobe levels of  $-24$  dB and  $-21$  dB at resonant frequencies. A noticeable difference that is greater than 20 dB between co-polarization and cross-polarization is observed. The dimensions of the antenna are  $56\text{ mm} \times 32\text{ mm} \times 0.508\text{ mm}$ . There is an excellent similarity between the simulated and measured results.

## 1. INTRODUCTION

In multi-band applications, different frequency bands of the antenna are commonly obtained by incorporating several sub-arrays working at specific frequencies, which can introduce undesirable noise among existing bands due to the antenna's space limitations. Furthermore, it introduces interference between the two frequencies of dual band antennas if the two signals are not separated properly. The effective integration of various essential RF front-end components on the same board would be a highly efficient solution to such challenges. Filters and antennas are the significant components in any radio frequency front-end system. Proper integration of these two can considerably increase the selective band of frequencies, gain stability, unwanted band rejection, and system efficiency [1]. Researchers achieved good frequency selectivity, efficiency, and a wide bandwidth by using integrated filter designs and antennas [2, 3]. Wide-bandwidth filtering antennas have also become important in base station applications [4]. Filtering antennas with narrow band pass response are beneficial in 5G and millimeter wave systems [5]. Substrate integrated waveguide (SIW) technology has recently acquired critical importance in the design of filtering antennas [6–8]. Slotted SIW antennas feature unique properties such as high-directional beam formation as well as low level side lobes and

---

*Received 3 February 2022, Accepted 31 March 2022, Scheduled 15 April 2022*

\* Corresponding author: Ayyadevara Murali Dhara Vitala Naga Maruti (marutianucet78@gmail.com).  
The authors are with the Acharya Nagarjuna University, Guntur, Andhra Pradesh, India.

cross-polarization. SIW based slot array antennas have become critical in 5G, millimeter wave, Tetra Hertz, and a variety of other high frequency range applications [9]. Previous research has presented SIW antennas with an array of longitudinal slots for reduced mutual coupling, low cross polarization, wide bandwidth, and low side lobe level [10–12]. The transverse current flowing through the wave guide induces an electric field in the slot. SIW does not require a complex feed network to excite the slots of an antenna with a waveguide feed system. Hence, it offers the elimination of radiation losses as well as cross coupling issues. The slot position determines the amount of impedance introduced. It also has an impact on the amount of energy emitted by the slot [13, 14]. The antenna proposed is fed via a microstrip to a SIW taper. The tapered microstrip transition used in this work has already been largely adopted in research as it offers excellent performance [15].

Complementary split-ring resonators are used in the development of band-pass filters to improve efficiency and achieve acceptable properties. With the combination of SIW technology and CSRR on a single planar substrate, it is possible to create a simple band pass filter with an elevated quality factor for wide band communication applications [16]. It has been confirmed that when CSRRs are etched on the radiating part of planar communication, signal transmission is excluded in the surrounding area of their resonant frequency, avoiding unwanted signals [17]. Various methods have been presented in previous research, and it is possible to predict the resonant frequency of a CSRR structure from its geometrical parameters [18].

The organization of the work is as follows. First, the CSRR structures of calculated dimensions for the desired frequencies are designed. Then CSRRs of the same dimensions are etched on the SIW antenna to build band pass filters. These band pass filters are followed by an array of longitudinal slots designed for preferred frequencies. Section 2 goes over the parameters and design in detail. The results of the simulation and measurements are presented in Section 3.

## 2. ANTENNA DESIGN

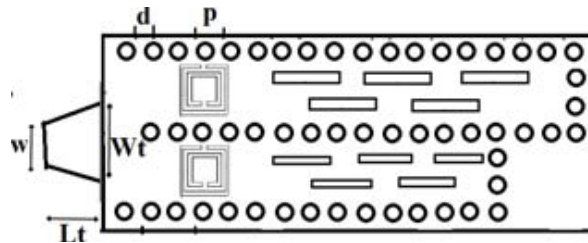
### 2.1. Basic SIW Antenna Design

Figure 1 depicts the proposed slotted SIW fed waveguide array antenna structure with CSRRs etched on the top plane of the SIW structure. The necessary and significant specifications for designing a SIW antenna with the required performance are the diameter of vias  $d$ , the space between the centers of two adjacent vias  $p$ , the gap between the rows of vias holes  $a$  and the  $d/p$  ratio. The height of the substrate should be as small as possible to minimize radiation losses. RT/Duroid 5880 material with  $\epsilon_r = 2.2$ , and a thickness  $h = 0.508$  mm is used. The diameter  $d$  and the separation of vias  $p$  must be chosen such that radiation leakage and other losses are minimized. The diameter of the vias is chosen to be less than  $\lambda_g/5$ , where  $\lambda_g$  is the guided wavelength. The fundamental design conditions are defined by Equations (1) through (4), from [13].

$$W_{eq} = \frac{C}{2f\sqrt{\epsilon_r}} \quad (1)$$

where  $f$  is the resonant frequency,  $c =$  velocity of light.

$$0.05 < \frac{p}{\lambda_c} < 0.25 \quad (2)$$



**Figure 1.** Proposed longitudinal slots array antenna fed by SIW.

$$0.5 < \frac{d}{p} < 0.8 \quad (3)$$

$$W_{\text{SIW}} = W_{eq} + \frac{d^2}{0.95p} \quad (4)$$

where  $W_{\text{siw}}$  = Width of the SIW antenna;  $W_{eq}$  = Equivalent width of antenna;  $\lambda_c$  = Cut off wavelength.

## 2.2. Microstrip to SIW Transition Taper Design

The microstrip taper is the most common method for transition from microstrip to SIW. It has a wideband operation and low return loss. It connects a microstrip of width  $W$  and the SIW of width  $W_s$ , so that both have the same impedance at the desired frequency. The length of the taper is determined primarily by the difference in microstrip line and SIW widths. In the millimeter band, for  $\epsilon_r = 2$  to 10, where widths are generally close, and a taper with a length  $\lambda_g/4$  is acceptable. Taper length should be multiples of  $\lambda_g/4$  as in Eq. (5) as given in [13].

$$L_t = \frac{n * \lambda_g}{4} \quad \text{Where } n = 1, 2, 3... \quad (5)$$

In this design, the taper length  $L_t = 7.8$  mm. Mathematical procedure in [15] can be used to calculate taper widths; microstrip width,  $W = 1.4$  mm and taper width on the SIW side,  $W_t = 2.2$  mm. The full specifications of the proposed antenna are tabulated in Table 2.

## 2.3. Band Pass Filter Design

The structure of the CSRR used in the band pass filter design is as shown in Figure 2(a) and consists of a pair of split resonating rings. CSRR incorporated into SIW offers an excellent passband around the center frequency of the SIW structure. The resonant frequency of the CSRR is given by Eq. (6),

$$f_{\text{CSRR}} = \frac{1}{2\pi\sqrt{LrCr}} \quad (6)$$

Here,  $Cr$  and  $Lr$  represent the self capacitance of the rings and their mutual inductance, respectively. Any analytical method can be used to calculate the dimensions of the CSRR at the specified frequency. Many approaches have been presented in past research to find the dimensions of the split rings [17, 18]. The optimal dimensions are selected using a parametric analysis. First, the values are calculated using different past research methods. All the techniques gave the same numerical values. Finally, the parametric studies of the proposed CSRRs are done using CST studio software to improve accuracy. They are tabulated in Table 1.

**Table 1.** CSRR dimensions.

S.No.	Parameter	At 10.2 GHz	At 16.4 GHz
1	Outer length ( $s$ )	3.6 mm	3.1 mm
2	Inner length ( $b$ )	2.0 mm	1.1 mm
3	Split gap ( $g$ )	0.3 mm	0.3 mm
4	Patch thickness ( $t$ )	0.3 mm	0.4 mm
5	Gap between rings ( $w$ )	0.5 mm	0.6 mm

The designed SIW band pass filter for the specified frequency is shown in Figure 2(b), and the equivalent circuit of the filter is depicted in Figure 2(c). The filters are designed such that they allow signals only in corresponding frequency bands around the centre frequencies. The resonant behavior of the simulated filters at two resonant frequencies is presented in Figures 3(a) and 3(b). From the plots, it is clear that the filters exhibit a passband around the desired frequencies and reject any signal. It can be seen that the center frequency of the upper band pass filter is 10.6 GHz in the X-band, and the passband return loss is better than 21 dB. The center frequency of the lower band pass filter is 16.5 GHz in the Ku-band.

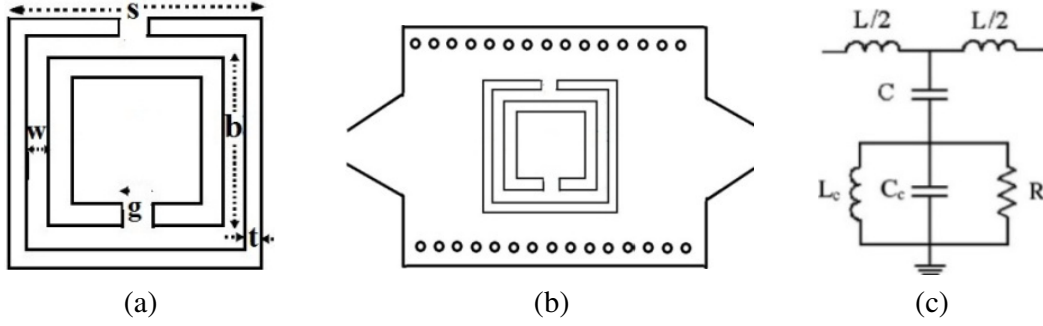


**Figure 2.** (a) CSRR layout. (b) Band pass filter design. (c) BPF equivalent circuit.

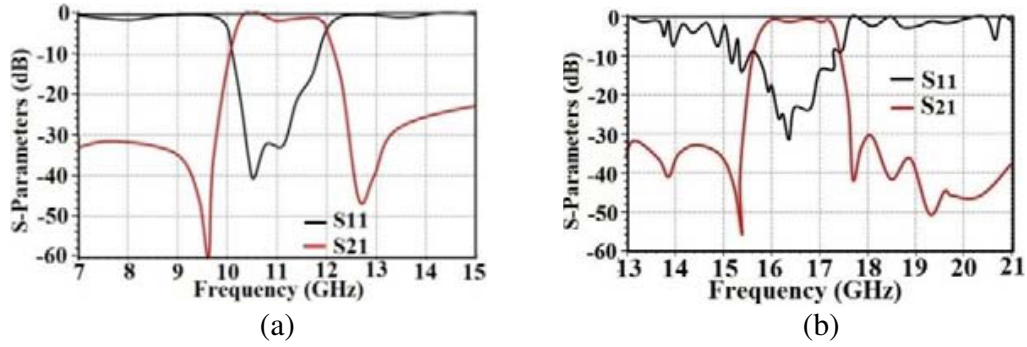


**Figure 3.** Simulated response, (a) upper BPF (X-band), (b) lower BPF (Ku-band).

#### 2.4. Slots Array Design

A slot array antenna is used to manage signal transmission or reception. The top layer of SIW has five longitudinal slots etched on it. The length of the slot is calculated using Equation (6) from [14].

$$l = \frac{\lambda_0}{\sqrt{2(1 + \epsilon_r)}} \quad (7)$$

The separation between the centers of the slots is  $\lambda_g/2$ . The width of the slot  $b$  was chosen to be less than  $\lambda_g/20$ ,  $b = 0.7$  mm. The spacing between the centers of the slots  $x$  is chosen as half of the guided wave length, such that the slots will be fed in phase. The distance between the last slot and the non-radiating edge  $z$  will also have an effect on the performance, and it is commonly assumed to be  $3\lambda_g/4$ .

A slot displacement is considered as a gap that separates the center of a slot from the center line of the wave guide broad wall. The slot displacement  $y$  is selected to minimize interference and optimized to make it resonant at the centre frequency. The slots should be arranged in an alternating pattern about the center line. Then, all slots will radiate in phase and therefore offer high effectiveness. The slots are equally spaced from the center line for uniform power division. The slot offset gap is given by Equation (7) given in [12].

$$y = \frac{W_{\text{siw}}}{\pi} \sqrt{\sin^{-1} \left[ \frac{1}{NG} \right]} \quad (8)$$

where

$$G = 2.09 * \frac{W_{\text{siw}}}{h} * \frac{\lambda_g}{\lambda_0} * \left[ \cos \left( 0.464\pi * \frac{\lambda_0}{\lambda_g} \right) - \cos(0.464\pi) \right]^2 \quad (9)$$

$N$  = No. of slots.  $W_{\text{siw}}$  = Width of the slot antenna  $h$  = thickness of the antenna.

After finding the value of  $y$  using this equation, it is then optimized to enhance the performance of the structure. Optimization of  $y$  for accurate resonance is shown in Figures 4(a) and 4(b).

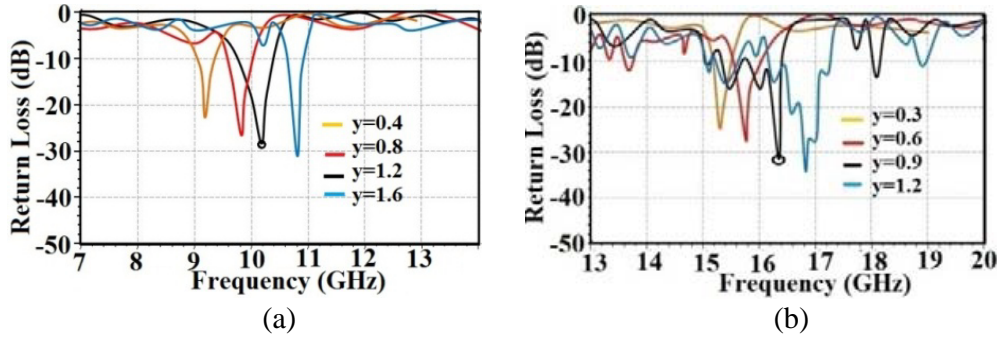


Figure 4. Optimization of displacement  $y$  for (a) 10.3 GHz, (b) 16.2 GHz.

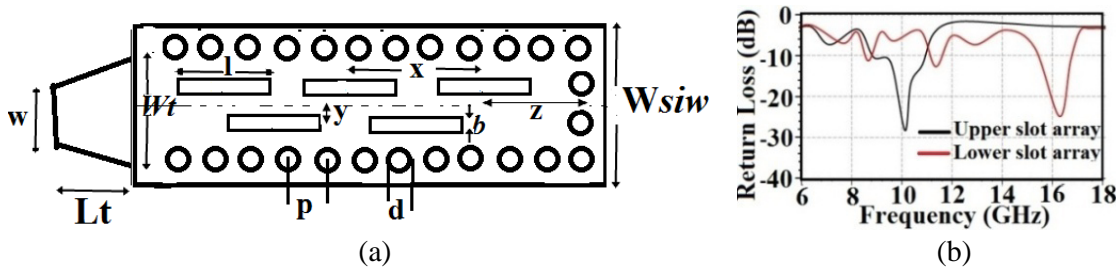


Figure 5. (a) Slot array layout. (b) Resonance of slot array antenna.

The calculated and optimized values differ slightly. The final values of  $x$ ,  $y$ , and  $z$  are chosen so that the antenna resonates at both frequencies with the best possible performance. The slot array antenna layout is shown in Figure 5(a). The parameters of the antenna calculated for both the frequencies are presented in Table 2. The resonant behavior of the slot array antenna is depicted in Figure 5(b). It concludes that the antenna exhibits good response at the desired frequencies.

Table 2. Slot array dimensions.

S.No.	Parameter	At 10.2 GHz	At 16.4 GHz
1	Slot length ( $l$ )	9.2 mm	7.1 mm
2	Slot width ( $b$ )	0.7 mm	0.6 mm
3	Slot displacement ( $y$ )	0.9 mm	1.2 mm
4	Inter-element spacing ( $x$ )	7.8 mm	5.9 mm

### 3. SIMULATION AND EXPERIMENTAL RESULTS

A structure is fabricated to test and validate for the intention. Figure 6 presents the fabricated antenna on a Rogers Duriod 5880 substrate. The full design specifications of the antenna to satisfy the conditions at both frequencies are shown in Table 3 below. The equivalent width of the SIW at 10.3 GHz is 11.3 mm while at 16.2 GHz it is 9.21 mm.

The return loss is measured using a Vector Network Analyzer. The simulated and measured return losses are shown in Figure 7(a). The plot shows that the antenna is resonant at 10.3 GHz and 16.2 GHz in the simulation. The fabricated structure resonates at 10.2 GHz and 16.4 GHz. The simulation and measurement findings differ slightly, because of the effect of connectors, fabrication issues, and testing conditions. At 10.2 GHz, the return loss is  $-33$  dB and  $-30$  dB at 16.2 GHz, for fabricated structure. The bandwidth is 1.9 GHz (9.2 to 11.1, 18.2%), and at 16.2 GHz, the bandwidth is 2.2 GHz (15.9 GHz to 18.1 GHz, 13.5%). All the results are tabulated in Table 4.

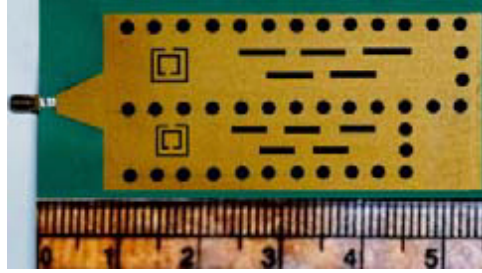
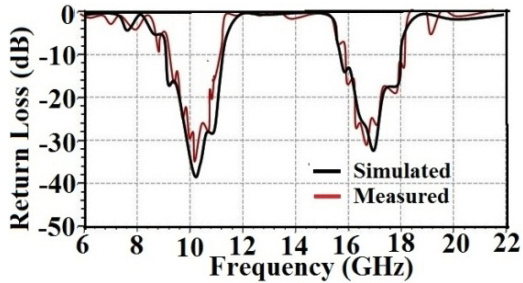
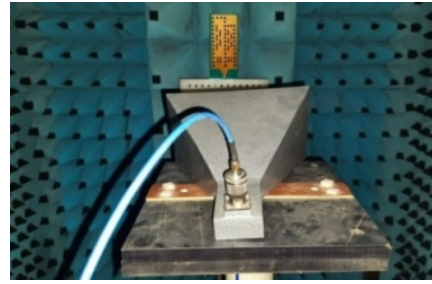


Figure 6. Fabricated antenna.



(a)



(b)

Figure 7. Proposed antenna. (a) Return loss comparison. (b) Gain measurement setup.

Table 3. Proposed antenna specifications.

S.No	Parameter	Value
1	Vias diameter ( $d$ )	1.8 mm
2	Separation between centers of vias ( $p$ )	2.8 mm
5	Taper length ( $L_t$ )	7.8 mm
6	Taper width on SIW ( $W_t$ )	2.2 mm
7	Taper width on feed side ( $W$ )	1.4 mm

Table 4. Comparison of simulated and fabricated antenna results.

S.No	Parameter	Simulated	Measured	Simulated	Measured
	Frequency	10.3 GHz	10.2 GHz	16.7 GHz	16.9 GHz
1	Gain	12.1 dB	11.6 dB	11.9	11.2 dB
2	Bandwidth	2.2	1.9 GHz	2.6	2.2 GHz
3	Return loss	-38 dB	-33 dB	-34 dB	-30 dB
4	Side lobe level	-24 dB	-21 dB	-22 dB	-20 dB

Gain and radiation patterns measurement setup of the antenna in an anechoic chamber is depicted in Figure 7(b). The gain is unidirectional with considerably low side lobes. Figures 8(a) and 8(b) show the co-polarizations of the  $E$ -plane and  $H$ -plane of the antennas, respectively. Cross polarizations of  $E$  plane and  $H$ -plane of the antenna at both frequencies are depicted in Figures 8(c) and 8(d). The radiation patterns are symmetrical at 10.2 GHz and slightly inclined at 16.4 GHz. They conclude that the radiation in the desired direction exceeds much of the radiation in unwanted directions. These

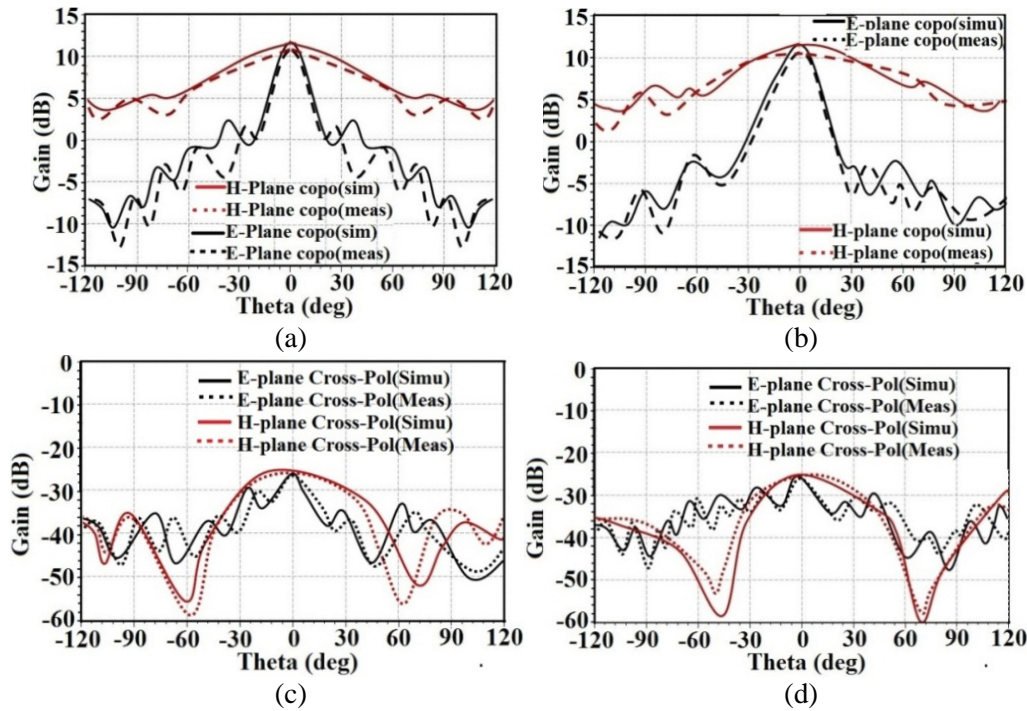


**Figure 8.** (a) Co-polarization at 10.2 GHz. (b) Co-polarization at 16.4 GHz. (c) Cross-polarization at 10.2 GHz. (d) Cross-polarization at 16.4 GHz.

figures reveal that the proposed antenna maintains excellent isolation between the cross-polarization and co-polarization. They differ by more than 20 dB in both the *E* and *H* planes. The beam efficiency, which is defined as a function of gain and side lobes, is found to be 69% and 64%, respectively.

Some of the past relevant publications on filtering antennas along with the present work are tabulated in Table 5. Each work has an excellent conceptual foundation and delivers good results that are above the performance threshold. The designs in [3] and [4] offer excellent bandwidth at lower frequencies, while [5] offers appreciable gain and bandwidth for 5G applications. The proposed array employs a simple design to attain the optimum radiation characteristics. It exhibits high gain and wide bandwidth.

**Table 5.** Comparison of present work and past research work on filtering antennas.

S.No	Ref.No.	Year	Frequency (GHz)	Gain (dB)	Bandwidth
1	[3]	2020	3	9.7	37.1%
2	[4]	2020	2.4	8.5	63%
3	[5]	2020	28	15	20%
4	[6]	2021	2.8	6.76	4.3%
5	[7]	2021	5.4	5.3	7.64%
6	[8]	2019	30	7.57	4.4%
7	Present work	—	10.2	11.6	18.2%
			16.4	11.2	13.5%

#### 4. CONCLUSION

SIW-CSRR band pass filters and slot array antennas were used to create a filtering antenna for X and Ku band applications. In dual band mode, band pass filters are designed to operate at chosen center frequencies and provide desirable separation between two frequencies. The unwanted range signals are rejected by the band pass filters. The slot array antenna performs the functions of radiation or reception. By optimizing significant parameters, the structure was made to resonate at the desired centre frequencies. The array is made of RT Duroid 5880 dielectric material and measures  $56 \text{ mm} \times 32 \text{ mm} \times 0.508 \text{ mm}$  in size. The antenna is fed via a microstrip to a SIW taper. The antenna is resonant at 10.2 GHz and 16.4 GHz. It exhibits gains of 11.6 dB at 10.2 GHz and 11.2 dB at 16.4 GHz. The bandwidth is 1.9 GHz and 2.2 GHz at 10.2 GHz and 16.4 GHz, respectively. There is an appreciable resemblance between the simulated and fabricated antennas. It is not necessary to add any additional circuitry to increase the bandwidth. If necessary, the gain can be increased further by increasing the number of slots or by connecting such antennas in parallel dimensions.

#### REFERENCES

1. Mao, C. X., Y. Zhang, X. Y. Zhang, P. Xiao, Y. Wang, and S. Gao, "Filtering antennas: Design methods and recent developments," *IEEE Microwave Magazine*, Vol. 22, No. 11, 52–63, 2021.
2. Liang, G.-Z., F.-C. Chen, H. Yuan, K.-R. Xiang, and Q.-X. Chu, "A high selectivity and high efficiency filtering antenna with controllable radiation nulls based on stacked patches," *IEEE Transactions on Antennas and Propagation*, Vol. 70, No. 1, 708–713, 2022.
3. Zhang, Y.-M., S. Zhang, G. Yang, and G. F. Pedersen, "A wideband filtering antenna array with harmonic suppression," *IEEE Transactions on Microwave Theory and Techniques*, Vol. 68, No. 10, 4327–4339, 2020.
4. Dng, C. F., Z. Y. Zhang, and M. Yu, "Simple dual-polarized filtering antenna with enhanced bandwidth for base station applications," *IEEE Transactions on Antennas and Propagation*, Vol. 68, No. 6, 4354–4361, 2020.
5. Yang, S. J., Y. M. Pan, L.-Y. Shi, and Z. Y. Zhang, "Millimeter-wave dual-polarized filtering antenna for 5G applications," *IEEE Transactions on Antennas and Propagation*, Vol. 68, No. 7, 5114–5121, 2020.
6. Wang, H.-Y., G. Zhao, R.-Y. Li, and Y.-C. Jiao, "A low-profile half-mode substrate integrated waveguide filtering antenna with high frequency selectivity," *Progress In Electromagnetics Research Letters*, Vol. 99, 35–43, 2021.
7. Xie, H. Y., B. Wu, Y.-L. Wang, C. Fan, J.-Z. Chen, and T. Su, "Wideband SIW filtering antenna with controllable radiation nulls using dual-mode cavities," *IEEE Antennas and Wireless Propagation Letters*, Vol. 20, No. 9, 1799–1803, 2021.
8. Hua, C., X. Jin, and M. Liu, "Design of compact vertically stacked SIW end-fire filtering antennas with transmission zeros," *Progress In Electromagnetics Research Letters*, Vol. 87, 67–73, 2019.
9. Altaf, A., W. Abbas, and M. Seo, "A wideband SIW-based slot antenna for D-band applications," *IEEE Antennas and Wireless Propagation Letters*, Vol. 20, No. 10, 1868–1872, 2021.
10. Diman, A. A., et al., "Efficient SIW-feed network suppressing mutual coupling of slot antenna array," *IEEE Transactions on Antennas and Propagation*, Vol. 69, No. 9, 6058–6063, 2021.
11. Zheng, D., Y.-L. Lyu, and K. Wu, "Longitudinally slotted SIW leaky-wave antenna for low cross-polarization millimeter-wave applications," *IEEE Transactions on Antennas and Propagation*, Vol. 68, No. 2, 656–664, 2020.
12. El Misilmani, H. M., M. Al-Husseini, and K. Y. Kabalan, "Design of slotted waveguide antennas with low sidelobes for high power microwave applications," *Progress In Electromagnetics Research C*, Vol. 56, 15–28, 2015.
13. Kachhia, J., A. Patel, A. Vala, R. Patel, and K. Mahant, "Logarithmic slots antennas using substrate integrated waveguide," *International Journal of Microwave Science and Technology*, Vol. 2015, 1–11, 2015.

14. Farrall, A. J. and P. R. Young, "Integrated waveguide slot antennas," *IEEE Electronics Letters*, Vol. 40, 974–975, 2004.
15. Zamzam, K. and J. Bornemann, "New wideband transition from microstrip line to substrate integrated wave guide," *IEEE Transactions on Microwave Theory and Techniques*, Vol. 62, No. 12, 2983–2989, 2014.
16. Fu, W., Z. Li, P. Liu, J. Cheng, and X. Qiu, "Modeling and analysis of novel CSRRs-loaded dual-band band pass SIW filters," *IEEE Transactions on Circuits and Systems II: Express Briefs*, Vol. 68, No. 7, 2352–2356, 2021.
17. Soundarya, G. and N. Gunavathi, "Compact dual-band SIW band pass filter using CSRR and DGS structure resonators," *Progress In Electromagnetics Research Letters*, Vol. 101, 79–87, 2021.
18. Rayala, R. K. and S. Raghavan, "Artificial neural network based SIW band pass filter design using complementary split ring resonators," *Progress In Electromagnetics Research C*, Vol. 115, 277–289, 2021.